HIGHER HARMONIC CONTROL FOR TILTROTOR VIBRATION REDUCTION

Mark W. Nixon
U.S. Army Vehicle Technology Center
NASA Langley Research Center, MS 340
Hampton, Virginia 23681-0001
email address: m.w.nixon@larc.nasa.gov

Raymond G. Kvaternik
NASA Langley Research Center, MS 340
Hampton, Virginia 23681-0001
email address: r.g.kvaternik@larc.nasa.gov

T. Ben Settle
Bell Helicopter Textron, Inc.
Fort Worth, Texas 76101
email address: BSettle-BHTI@mcimail.com

Abstract. The results of a joint NASA/Army/Bell Helicopter Textron wind-tunnel test to assess the potential of higher harmonic control (HHC) for reducing vibrations in tiltrotor aircraft operating in the airplane mode of flight, and to evaluate the effectiveness of a Bell-developed HHC algorithm called MAVSS (Multipoint Adaptive Vibration Suppression System) are presented. The test was conducted in the Langley Transonic Dynamics Tunnel using an unpowered 1/5-scale semispan aeroelastic model of the V-22 which was modified to incorporate an HHC system employing both the rotor swashplate and the wing flaperon. The effectiveness of the swashplate and the flaperon acting either singly or in combination in reducing 1P and 3P wing vibrations over a wide range of tunnel airspeeds and rotor rotational speeds was demonstrated. The MAVSS algorithm was found to be robust to variations in tunnel airspeed and rotor speed, requiring only occasion-al on-line recalculations of the system transfer matrix.

Key words: active control, aeroelasticity, higher harmonic control, HHC, rotorcraft dynamics, tiltrotor, vibration

1. Introduction

Rotary-wing aircraft are prone to vibrations due to the intrinsic periodic nature of the airloads acting on the rotor blades. Tiltrotor aircraft operating in the airplane mode of flight are inherently less susceptible to vibrations than helicopters because the airflow through their rotors is predominantly axial rather than inclined. However, airframe vibration levels in tiltrotor aircraft are still typically greater than those in conventional propeller-driven fixed-wing aircraft. There are two principal sources of rotor-induced airframe vibration in a tiltrotor operating in the airplane mode of flight: (1) the aerodynamic interference between the rotor blades and the wing; and (2) the wake of the rotor impinging on the empennage. The circulation associated with a lifting wing and the streamline curvature induced by a finite-thickness wing create an azimuthally unsymmetric flow field through the rotor disc which results in oscillatory blade loads that are transmitted to the hub and down the mast into the airframe (pylon, wing, fuselage) as vibratory forces and moments at frequencies which are integer multiples of the blade passage frequency. The shed rotor wake also excites the airframe at the blade passage frequency. While these effects are present in conventional propeller-driven aircraft, they are more significant in tiltrotors because of the larger diameter of proprotors as compared to propellers. One approach to reducing proprotor-induced airframe vibrations is to actively control the vibrations at their source (the rotor) by introducing higher harmonic collective and cyclic blade pitch using the fixed-system swashplate to modify the blade aerodynamic loading in a manner which eliminates or at least reduces substantially the resultant rotor loads entering the airframe at the hub. The use of the rotor swashplate to actively control vibration in this way is generally referred to as higher harmonic control (HHC). However, it is clear that HHC systems for vibration reduction can also utilize airframe control surfaces such as flaps, ailerons, elevators, and rudders, airframe-mounted devices such as seismic masses and force actuators, and blade-mounted devices such as actively-controlled pitch links and control surfaces.

HHC methods based on using an actively-controlled swashplate have the longest research history and have received the most attention. Concise summaries of the work dealing with this approach may be found in references 1-3. The crucial role played by the vibration control algorithm in any practical implementation of HHC is well recognized and considerable attention has also been devoted to this aspect of helicopter HHC systems (see, for example, refs. 4-7). Based on the results of these studies, higher harmonic control using an actively-controlled swashplate has been judged to be one of the most effective vibration control techniques applicable to helicopters. Some of the most significant findings associated with the HHC studies reported in the literature are: (1) The major oscillatory rotor loads transmitted into the nonrotating system can be effectively eliminated by oscillating the swashplate at a single harmonic of the rotor rotational speed; (2)

Simultaneous reduction of several components of the vibratory hub loads is possible due to superposition of the effects of the individual harmonic pitch oscillations; (3) HHC has a negligible effect on rotor performance; (4) HHC has only a small effect on blade loads; (5) Pitch link loads can be significantly increased; and (6) An adaptive HHC system requires a Kalman Filter to identify the system transfer function.

Tiltrotor aircraft operate in both the helicopter and airplane modes of flight. Because tiltrotors are designed to spend most of their flight time in the airplane mode, primary interest for this type of rotorcraft is on reducing airframe vibrations when operating in the airplane mode of flight. While much of the HHC research conducted for helicopters is probably directly applicable to tiltrotors operating in the helicopter mode of flight, it is not clear how much of that work (if any) is directly applicable to tiltrotor aircraft operating in the airplane mode of flight.

The purpose of this paper is to summarize the results of a joint NASA/Army/Bell-Helicopter investigation which was conducted in the Langley Transonic Dynamics Tunnel to assess the potential of HHC for reducing vibrations in tiltrotor aircraft operating in the airplane mode of flight, and to evaluate the effectiveness of the MAVSS control algorithm. The current paper is an abbreviated version of a more detailed account of this study which may be found in reference 8. The wind-tunnel study employed a 1/5-scale semispan aeroelastic model of the V-22 which was modified to incorporate an HHC system consisting of the rotor swashplate and the wing control surfaces (flap and aileron) acting together as a single control surface. Three high-frequency servo-controlled hydraulic actuators were employed to control the swashplate and a fourth actuator was used to control the flaperon. The effectiveness of the rotor swashplate and the wing flaperon in reducing vibrations was investigated both singly and in combination over a wide range of tunnel airspeeds and rotor rotational speeds.

2. Experimental Setup

2.1 Model

The model used in the investigation is a modified version of a 1/5-scale semispan aeroelastic model which was used to support the preliminary and full-scale design phases of the V-22 aircraft (Ref. 9). Upon completion of that series of tests, the Navy transferred the model to NASA Langley under a loan agreement to be used as the experimental testbed of a tiltrotor aeroelastic research program which was initiated at Langley in 1994. The tiltrotor testbed has been designated the Wing and Rotor Aeroelastic Testing System (WRATS). The WRATS tiltrotor model as installed in the Langley Transonic Dynamics

Figure[1]. Model in NASA Transonic Dynamics Tunnel.

Tunnel for this study is shown in Figure [1]. Modifications to the baseline model required for the active controls testing included the replacement of the electric control actuators with high-frequency hydraulic servo-actuators to drive the swashplate and a new servo-controlled wing flaperon. The model also incorporated a new, elastically-tailored, graphite-epoxy wing spar. This spar was used in an earlier aeroelastic stability investigation (Ref. 10) unrelated to the present study and left on the model for convenience.

The model has a length scale factor of 1/5 and was designed to maintain full-scale values of the Froude, Lock, and Strouhal numbers when operated in air (Ref. 9). The wing and rotor are aeroelastically scaled; the pylon is only dynamically scaled. The fuselage is rigid and only maintains the scaled external aerodynamic shape. The model is attached to a support structure which is effectively rigid, its lowest frequency being well above any important elastic mode frequency of the model. Simulation of the distributed wing beamwise, chordwise, and torsional stiffness is provided by means of a hollow, elastically-tailored, composite spar having chordwise flanges. The 4.6-foot long spar, which lies along the calculated elastic axis of the wing, has segmented, nonstructural, aluminum aerodynamic fairings which provide the spanwise distribution of airfoil contour. To provide surface continuity over the wing lifting surface, the gap between the segments at the surfaces is filled by strips of foam rubber. The wing-tip-mounted pylon contains the transmission and gearbox components for the rotor drive system, the lower part of the mast, and the swashplate control system. Because these internal components can be treated as rigid, the pylon was scaled dynamically so as to preserve its overall mass and inertia. The pylon is attached to the wing by means of a “racetrack” spring which simulates the combined stiffness of the full-scale conversion actuator and downstop-lock mechanism.

The 3-bladed, 7.6-foot diameter rotor has a gimbaled hub which is connected to the mast by a constant velocity joint (2 coincident universal joints). The rotor yoke has 2.5 degrees of built-in precone and is flexible to allow the blade coning angle to adjust under aerodynamic and centrifugal loading. The blades have a nonlinear distribution of built-in twist with an overall root-to-tip twist of 47.5 degrees (leading edge down).

2.2 Active Swashplate and Flaperon Hardware

A total of four high-frequency hydraulic servo-actuators were used in the control system, one to drive the flaperon and three to drive the swashplate. The swashplate actuators were arranged in a 'milkstool' configuration around the nonrotating part of the swashplate. These actuators were used to input the usual steady pilot commands as well as the higher harmonic swashplate excitations called for by the active control algorithm. These servo-actuators were made up of four Oildyne 3/4" hydraulic cylinders with Moog Series 32 servo-valves which provided a bandwidth in excess of 50 Hz at 3000 psi supply pressure. The swashplate servo-valves were located inside the pylon near their corresponding actuators. The flaperon actuator and its servo-valve were located inside the fuselage fairing at the root of the wing. Harmonic swashplate actuation was limited to ± 2 degrees for each of the three control angles.

The new flaperon needed for active controls testing was designed to withstand the dynamic loads associated with oscillating the flaperon up to ± 6 degrees at 50 Hertz. The flap and aileron which comprise the flaperon are identical, each having a five-inch chord and a span half the length of the wing. The flaperon is attached to a torque tube which is positioned along the 3/4-chord of the wing and supported by hanger bearings. Harmonic excitations of the flaperon were limited to ± 3 degrees for most of the test.

2.3 Feedback Signals and Instrumentation

Feedback signals for the control system were developed from the measured responses of the pylon/wing system. The suite of candidate responses included wing root strain gages (beam, chord, and torsion) and three pylon accelerations. Analog response signals of interest were digitized and a real-time harmonic analysis was performed to extract the response at the harmonic frequency (or frequencies) of interest. The cosine and sine components of these harmonics were then input to the MAVSS HHC algorithm which calculated and updated the actuator signals required to minimize the vibration.

The instrumentation used for response feedback to the control system were wing strain gages and pylon accelerometers. Wing bending and torsion moments are calibrated to standard strain-gage bridges located near the wing root. The beam and chord strain gages are located 17.0 inches out from the root and the torsion strain gages are located 23.0 inches out from the root. The wing bending and torsion gages were the sensors selected most often for feedback. A number of other measurements were monitored and recorded either to trim the rotor or for flight safety including: gimbal flapping, the downstop spring load, pitch-link load (one pitch link instrumented), and blade flapwise and chordwise bending at five spanwise locations (one blade instrumented). Blade torsion was not measured.

3. Higher Harmonic Active Vibration Control Algorithm

3.1 Overview of the Control Algorithm

The higher harmonic active vibration control algorithm employed in this study is implemented in a BHTI proprietary software system called the Multipoint Adaptive Vibration Suppression System (MAVSS). MAVSS is designed to minimize rotorcraft vibrations occurring at integer multiples of the rotor speed. For a three-bladed rotor system, the largest vibratory forces acting on the airframe occur at a frequency of three-per-rev (3P).

The MAVSS algorithm assumes that changes in the aircraft responses are linearly related to changes in control inputs through a system transfer matrix which represents a locally-linearized model of the measured aircraft dynamics. Should the algorithm detect that its (current) linearized model is no longer providing an adequate representation of the system dynamics, MAVSS re-identifies the transfer matrix on line. MAVSS operates in the rotor frequency domain in near real time. All data acquisition and commands are triggered by rotor position and thus MAVSS can remain synchronized with the rotor rotational speed, even if the rotor speed varies. Commands for the current rotor revolution are computed based on the measurements made on the last rotor revolution and its linearized model of the measured aircraft dynamics.

The deterministic controller on which MAVSS is based is obtained by minimizing a scalar performance index which includes the harmonic vibratory responses to be reduced, the HHC inputs necessary to effect the reduction, and the transfer matrix describing the dynamics of the system. Since both measured vibrations and actuator commands are included in the performance index, the system always tries to minimize both the measured vibrations and the work done by the actuators.

A simplified flowchart which indicates the major computational blocks in MAVSS is shown in Figure

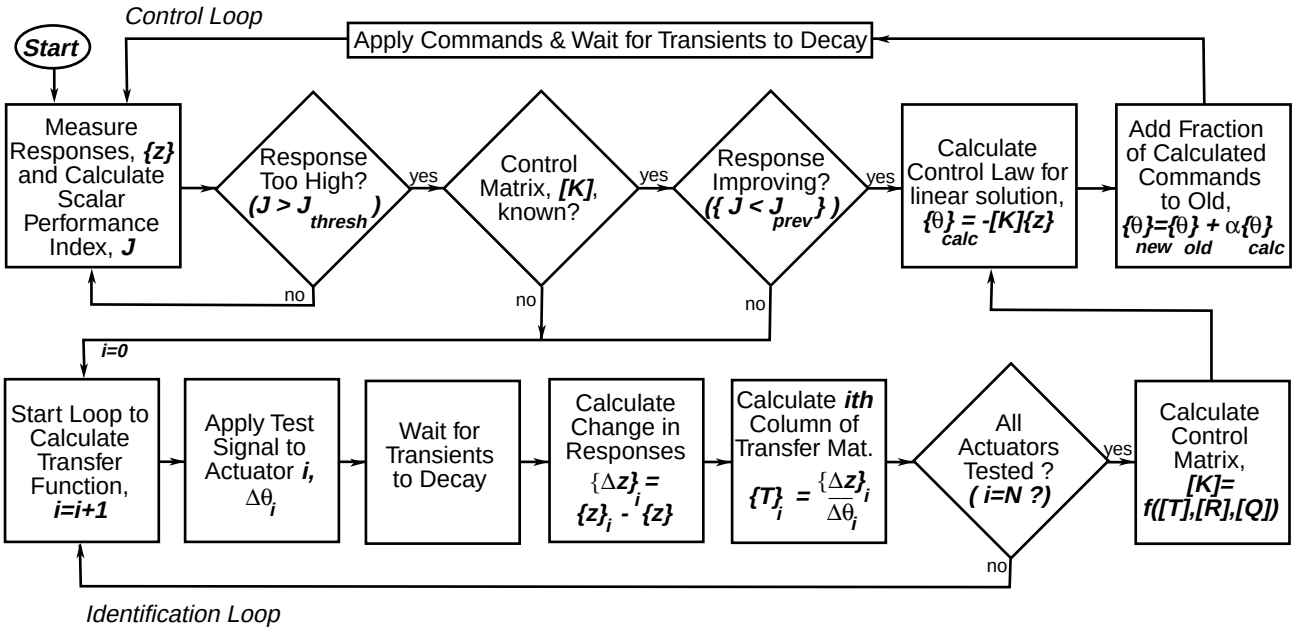

Figure [2]. Major computational blocks in MAVSS active vibration control algorithm.

[2]. To start the process, the system responses at the harmonics of interest (e.g., 3P) are measured and the performance index is calculated and compared to the threshold value of the index. The initial value of the index (*i=0*) should be well above the threshold value because no control has yet been applied. As MAVSS has no prior knowledge of the aircraft dynamics when it is first started, the control matrix *[K]* must be determined. MAVSS calculates this matrix by applying a known signal at the harmonic of interest to each of its control actuators in turn and then normalizing the resulting change in system vibrations by the applied signal. To account for the possibility of system nonlinearities, only a fraction of the calculated control change is added to the existing control and then applied to the actuators. The performance index is then recalculated using the new vibratory responses and compared to both its previous value and the threshold value. If the new index is smaller than the previous value but is still larger than the threshold value then a new set of control commands is calculated. Continuing in this manner, the index is driven down incrementally to just below its threshold value. Once the measured vibrations are below the threshold value, MAVSS simply maintains the latest set of commands and monitors the aircraft responses. Should the flight condition or forcing function change and the measured responses exceed the threshold, MAVSS uses the latest measured responses to calculate a new set of commands and applies them to the actuators. This cycle is repeated until the vibration level is driven back down to just below the specified threshold. Under ideal conditions, the transfer matrix should not need to be re-identified. Only major changes in the aircraft dynamics would warrant re-identification of the transfer matrix. Changes in the external forces themselves do not necessarily require re-identification.

3.1 Determination of the Transfer Matrix

The transfer matrix is based on M responses and N control actuators. Although M is generally equal to or greater than N, this is not necessary for the algorithm to work. A harmonic analysis is used to obtain the cosine and sine components of the response as:

$$\{Z_{ic}\}_n = \left\{ \frac{2}{K_s} \sum_{k=1}^{K_s} z_i(k\Delta\psi)\cos(nk\Delta\psi) \right\}, \quad i = 1, M \qquad (1)$$

$$\{Z_{is}\}_n = \left\{ \frac{2}{K_s} \sum_{k=1}^{K_s} z_i(k\Delta\psi)\sin(nk\Delta\psi) \right\}, \quad i = 1, M \qquad (2)$$

where $z_i(k\Delta\psi)$ represents the ith response signal at $k\Delta\psi$ position in the azimuth (proportional to time), n is the harmonic of interest (primarily 3P in the present study), K_s is the number of samples contained in the digitized response signal, and $\Delta\psi$ is the azimuth angle traveled by the reference blade in the time between samples. The test signals sent to the actuators to identify the transfer matrix are harmonics at the frequency of interest and do not have to be

harmonically analyzed. Let these signals be assembled in the column vectors $\{\Theta_{jc}\}_n$ and $\{\Theta_{js}\}_n$ for $j = 1, N$.

A ($2M$ x 1) vector of the change in response between the baseline response (subscript *base*) and the response to the test signal (subscript *test*) is given as

$$\begin{Bmatrix} \Delta Z_{ic} \\ \Delta Z_{is} \end{Bmatrix} = \begin{Bmatrix} Z_{ic} \\ Z_{is} \end{Bmatrix}_{test} - \begin{Bmatrix} Z_{ic} \\ Z_{is} \end{Bmatrix}_{base}, \quad i = 1, M \tag{3}$$

It should be pointed out that in this paper 'baseline response' means the current level of controlled vibrations and not the vibratory response with HHC off. The corresponding change in the control signal is given by:

$$\begin{Bmatrix} \Delta\Theta_{jc} \\ \Delta\Theta_{js} \end{Bmatrix} = \begin{Bmatrix} \Theta_{jc} \\ \Theta_{js} \end{Bmatrix}_{test} - \begin{Bmatrix} \Theta_{jc} \\ \Theta_{js} \end{Bmatrix}_{base}, \quad j = 1, N \tag{4}$$

The transfer matrix is then defined as the $2M$ x $2N$ matrix in the equation

$$\begin{Bmatrix} \Delta Z_{ic} \\ \Delta Z_{is} \end{Bmatrix} = \begin{bmatrix} \frac{\Delta Z_{ic}}{\Delta\Theta_{jc}} & \frac{\Delta Z_{ic}}{\Delta\Theta_{js}} \\ \frac{\Delta Z_{is}}{\Delta\Theta_{jc}} & \frac{\Delta Z_{is}}{\Delta\Theta_{js}} \end{bmatrix} \begin{Bmatrix} \Delta\Theta_{jc} \\ \Delta\Theta_{js} \end{Bmatrix}, i = 1, M, \; j = 1, N \tag{5}$$

which relates changes in control inputs to changes in system responses. Since the system is assumed to be linear, the following relationships are used to reduce the time needed to compute the matrix:

$$\frac{\Delta Z_{is}}{\Delta\Theta_{js}} = \frac{\Delta Z_{ic}}{\Delta\Theta_{jc}} \tag{6}$$

$$\frac{\Delta Z_{ic}}{\Delta\Theta_{js}} = -\frac{\Delta Z_{is}}{\Delta\Theta_{jc}} \tag{7}$$

3.2 Vibration Minimization

To minimize vibration it is desired to drive the total responses due to the rotor and the applied HHC toward zero. Similar to equation (3), the change in response associated with an applied HHC (subscript *con*) may be written as

$$\begin{Bmatrix} \Delta Z_{ic} \\ \Delta Z_{is} \end{Bmatrix} = \begin{Bmatrix} Z_{ic} \\ Z_{is} \end{Bmatrix}_{con} - \begin{Bmatrix} Z_{ic} \\ Z_{is} \end{Bmatrix}_{base}, \quad i = 1, M \tag{8}$$

and making use of the transfer matrix allows equation (8) to be written as

$$\begin{bmatrix} \frac{\Delta Z_{ic}}{\Delta\Theta_{jc}} & \frac{\Delta Z_{ic}}{\Delta\Theta_{js}} \\ \frac{\Delta Z_{is}}{\Delta\Theta_{jc}} & \frac{\Delta Z_{is}}{\Delta\Theta_{js}} \end{bmatrix} \begin{Bmatrix} \Theta_{jc} \\ \Theta_{js} \end{Bmatrix}_{con} = \begin{Bmatrix} Z_{ic} \\ Z_{is} \end{Bmatrix}_{con} - \begin{Bmatrix} Z_{ic} \\ Z_{is} \end{Bmatrix}_{base} \tag{9}$$

Now since it is desired to minimize the response after the control is applied, the quantity that must be minimized is

$$\begin{aligned} z_k &= T_{kl}\theta_l + (z_b)_k \\ &= \begin{bmatrix} \frac{\Delta Z_{ic}}{\Delta\Theta_{jc}} & \frac{\Delta Z_{ic}}{\Delta\Theta_{js}} \\ \frac{\Delta Z_{is}}{\Delta\Theta_{jc}} & \frac{\Delta Z_{is}}{\Delta\Theta_{js}} \end{bmatrix} \begin{Bmatrix} \Theta_{jc} \\ \Theta_{js} \end{Bmatrix}_{con} + \begin{Bmatrix} Z_{ic} \\ Z_{is} \end{Bmatrix}_{base} \end{aligned} \tag{10}$$

$$i = 1, M; \; j = 1, N; \; k = 1, 2M; \; l = 1, 2N$$

where z is a ($2M$ x 1) vector that represents the response associated with the current control signal (M cosine components and M sine components). Notice at this point in the formulation that it was advantageous to convert to standard indicial notation with new indices k and l running twice the number of i and j. From this point forward, k is understood to cycle through M cosine and M sine components of the response points ($2M$ total) and l is understood to cycle through the N cosine and N sine components of the control points ($2N$ total).

It should be noted that the development given above has implicitly assumed only one harmonic of interest for vibration reduction. If there are two harmonics targeted for reduction, there will be two cosine terms and two sine terms for each physical actuator and/or response point and the size of all matrices and vectors doubles.

3.3 Performance Characterization

A scalar performance index is now introduced as

$$J = z_k^T R_{kk} z_k + \theta_l^T Q_{ll} \theta_l \tag{11}$$

where z is the response associated with the current control signal, θ is the current control signal, and R and Q are diagonal weighting matrices used to scale the performance index:

$$R_{kk} = \frac{1}{(z_m)_k^2} \tag{12}$$

$$Q_{ll} = \frac{1}{(\theta_m)_l^2} \tag{13}$$

where the $(z_m)_k$ are user-defined inputs which should reflect the target response level for the ith response point and the $(\theta_m)_l$ are user-defined inputs which should reflect a maximum allowable control input for the lth actuator.

Combining equations (10) and (11) gives the performance index desired for minimization as

$$J = (T_{kl}\theta_l + (z_b)_k)^T R_{kk} (T_{kl}\theta_l + (z_b)_k) + \theta_l^T Q_{ll} \theta_l \tag{14}$$

where T is the transfer matrix, θ is the control signal, and z_b is the baseline response. The value of the

control signal which will minimize J can be determined through expansion of the above expression and taking the derivative of J with respect to the control input θ:

$$(\frac{\partial J}{\partial \theta})_l = (z_b)_k^T R_{kk} T_{kl} + T_{lk}^T R_{kk} T_{kl} \theta_l + Q_{ll} \theta_l = (0)_l \qquad (15)$$

from which the control input which will satisfy this expression is given as

$$\theta_l = -[T_{lk}^T R_{kk} T_{kl} + Q_{ll}]^{-1} [T_{lk}^T R_{kk} (z_b)_k] \qquad (16)$$

which may be written in control law form as:

$$\theta_l = -K_{lk} (z_b)_k \qquad (17)$$

where K is the control matrix. For a linear system, application of equation (17) gives a set of control signals which minimizes J. As mentioned earlier when discussing Figure [2], to account for any system nonlinearities, only a fraction of the calculated change in control signal is added to the existing control signal and applied to the actuators. This piecewise linear stepping is repeated until the threshold is reached.

4. Results And Discussion

Higher harmonic control was very effective in suppressing the fixed-system vibratory responses of the tiltrotor model in airplane mode. The MAVSS control system, when configured to reduce 3P harmonics of the wing loads, was generally able to reduce the wing beam, chord, and torsion load components simultaneously by 85 to 95 percent over the entire range of rotor speeds and tunnel airspeeds considered. Representative results are shown in Figure [3] for the case *M=3* (wing beam, chord and torsion load feedback equally weighted) and *N=4* (activation of both the swashplate and flaperon). The plot shows that with HHC turned off, the 3P vibratory loads increase with airspeed, and that the chordwise vibratory load is substantially higher than are the beam and torsion load components. The vibratory loads in the wing chord direction are larger than the wing beam and torsion load components because the chord component of load is affected mainly by the changes in rotor thrust (actually drag for a windmilling rotor) while the beam and torsion components are influenced primarily by the rotor inplane forces, and the vibratory components of rotor thrust tend to be much larger than the vibratory components of the rotor inplane forces. When the control system is activated, the 3P load in all three wing load components is shown to decrease significantly over the same range of airspeeds. The indicated load reductions vary from 85 to 95 percent of the corresponding uncontrolled values. These results are similar, in terms of magnitude of vibratory load

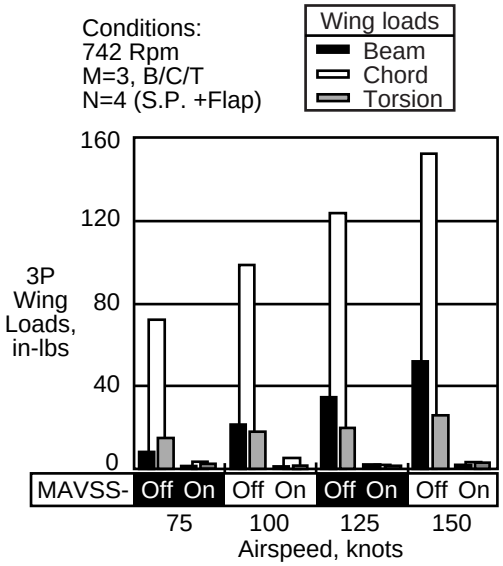

Figure [3]. 3P wing loads as a function of airspeed.

reduction, to those obtained for a model CH-47 3-bladed articulated rotor system in reference 11.

One aspect of the HHC system which needed to be investigated was the effect on the response associated with the number and choice of control points (actuators) used for input and the number and choice of response points (strain and acceleration measurements) used for feedback. Based on the principle of superposition for linear systems, one would expect that the number of control points should equal the number of response points. However, there are two reasons why this need not be the case for the present system: (1) the present system may be nonlinear; and (2) the response points considered may not be independent. As a simple example of the latter case, consider the vibration of a cantilevered wing with two response points for feedback and a single actuator control point. If two strain gages are both oriented to measure bending in the same direction, then a single actuator oriented in the same beam bending direction would likely have a high degree of success at reducing vibration at both locations. If the orientation of the response points considered are orthogonal, or nearly so, such that one gage measures primarily beam bending loads and the other primarily chord bending loads, then the actuator is likely to be much less effective in reducing at least one of those vibratory responses, no matter how the actuator is oriented with respect to those two directions.

Figure [4] shows the level of vibration reduction achieved in terms of a scalar load factor *F/F0* for several combinations of control points (*N*=1,3,4) and response points (*M*=1,2,3). This term represents a ratio of the total vibratory load with HHC on to that with HHC off, and *F* itself represents a resultant magnitude of the load components as given by

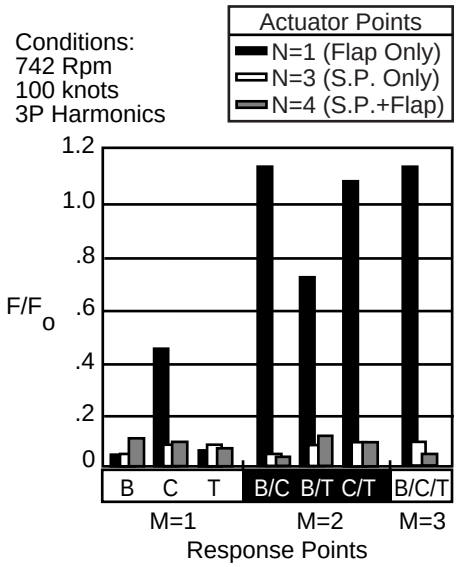

Figure [4]. Load factors for several cases of HHC.

$$F = \sqrt{\sum_{i=1}^{M} f_i^2} \qquad (18)$$

where each f is the load considered in the performance index corresponding to a particular case.

Figure [4] shows that the flaperon by itself (N=1) can be very effective at reducing vibration levels in a single load component, especially the beam and torsion loads. For the flaperon-only case, the chord load component was not reduced as much as the beam and torsion components because more amplitude of flaperon motion is required than was allowed in this test ($\pm$3 degrees limit). Results from an earlier test (Ref. 12) indicated that the flaperon-only case could lower the chordwise 3P load to about the same level as that associated with the beam and torsion components if given enough flap amplitude ($\pm$6 degrees). However, a flaperon-only controller was not effective at reducing vibration in multiple load components simultaneously.

The effectiveness of the controller in reducing multiple loads simultaneously greatly improves for the swashplate alone (N=3) and the swashplate plus flaperon together (N=4), as is shown in Figure [4]. The active control system is seen to have about the same level of effectiveness for the N=3 and N=4 setups no matter how many response points are considered for feedback, up to M=3. In general, it is observed that an order of magnitude reduction in the 3P loads is obtained when $N \geq M$. Figure [4] also shows that the reduction associated with use of the flaperon and swashplate together can be either more or less effective that the swashplate alone.

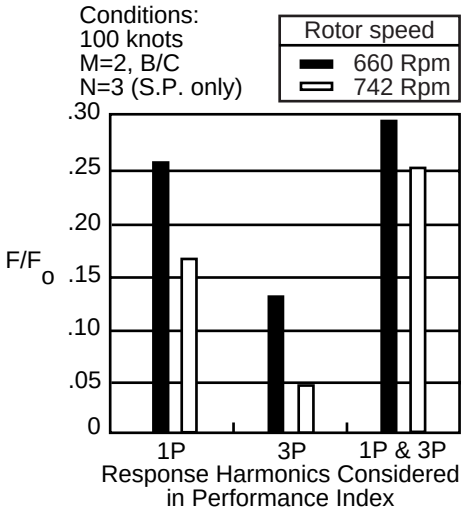

Figure [5]. Load factor associated with choice of harmonics in the performance index.

Figure [5] shows the load factor associated with the use of wing beam and chord load feedback and minimization of 1P loads, 3P loads, and combined 1P/3P loads, respectively. Two rotor speeds are considered, the model-scale design rotor speed for airplane mode cruise of 742 RPM and a rotor speed chosen to amplify the 1P loads, 660 RPM (11Hz) which is near the natural frequency of the wing fundamental chord mode. For the conditions considered, Figure [5] shows that 1P loads were reduced considerably (about 75-85%), although not as much as the 3P loads (about 85-95%). The combined 1P and 3P loads were reduced almost as much as the 1P loads alone (about 70-75%). These results demonstrate the ability of the HHC system to reduce multiple load com-ponents simultaneously using multiple HHC inputs.

In the present investigation, rapid changes in the model operating conditions (rotor speed and tunnel velocity) were used to evaluate the HHC algorithm for its effectiveness in adapting to changes in the system dynamics. Results of this part of the study showed that the algorithm is very robust with respect to adapting to rapid changes in either airspeed, rotor speed, or a combination of both, and reidentification of the system transfer matrix was rarely required. Under separate changes in airspeed (50 knots over a 10 second interval) and rotor speed (130 RPM over a 5 second interval), the algorithm did not need to reidentify the transfer matrix, but was still very effective at reducing vibrations using the initial transfer matrix which was identified at some nominal flight condition. In an attempt to exercise the portion of the algorithm which calls for a reidentification of the system transfer matrix, the airspeed and rotor speed were swept simultaneously at rates comparable to those noted above, and in a few cases the algorithm

did reidentify the transfer matrix. There was no significant degradation in the existing vibration during the process.

5. Conclusions

A joint NASA/Army/Bell Helicopter Textron wind-tunnel investigation was conducted to assess the potential of higher harmonic control (HHC) for reducing airframe vibrations in tiltrotor aircraft operating in the airplane mode of flight and to evaluate a Bell-developed HHC algorithm for tiltrotor vibration reduction. On the basis of the results shown, the following conclusions are indicated:

1) The HHC system employed was highly effective in reducing vibrations in the wing of the 3-bladed gimballed-rotor model tested. The HHC system was able to consistently reduce the 3P and 1P vibratory responses, either singly or in combination, by 75-95 percent.

2) Simultaneous reduction of several independent components of airframe vibration is possible because the effects of different higher harmonic pitch inputs can be superimposed. While the individual vibratory response of any of the three primary wing responses (beam, chord, or torsion) can be significantly reduced using an appropriate single actuator/sensor combination, multiple actuators and sensors must be used to effect the same level of reduction in several independent vibratory components simultaneously. In general, the number of actuators must be equal to or greater than the number of response sensors in order for the HHC to be effective in reducing multiple vibratory responses.

3) The HHC system was extremely robust with respect to its performance in the tracking of rapid changes in both the rotor speed and the airspeed, either singly or in combination.

4) The HHC transfer matrix, when identified at a nominal condition, was generally sufficient for a wide range of rotor speeds and tunnel velocities relative to those nominal conditions. Reidentification of the system transfer matrix was rarely required.

5) Despite the considerable differences in dynamic behavior and aerodynamic environment associated with tiltrotors and helicopters, a number of the results obtained in this study are similar to those obtained in studies of HHC for application to helicopters. This indicates that a considerable portion of the existing helicopter HHC technology base may be applicable to tiltrotors.

6. References

1. Nguyan, K. Q., "Higher Harmonic Control Analysis for Vibration Reduction of Helicopter Rotor Systems," University of Maryland Ph.D. Dissertation, UM-AERO-89-23, 1989.

2. Friedmann, P. P., "Rotary-Wing Aeroelasticity with Application to VTOL Vehicles," 31st AIAA/ASME /ASCE/AHS/ACS Structures, Structural Dynamics and Materials Conference, Long Beach, CA, April 2-4, 1990, pp. 1624-1670. (AIAA Paper 90-1115-CP).

3. Friedmann, P., "Rotary-Wing Aeroservoelastic Problems," AIAA Dynamics Specialist Conference, April 16-17, 1992, Dallas, TX, pp. 248-272. (AIAA Paper 92-2107-CP).

4. Molusis, J. A., Hammond, C. E., and Cline, J. H., "A Unified Approach to the Optimal Design of Adaptive and Gain Scheduled Controllers to Achieve Minimum Helicopter Rotor Vibration," 37th Annual Forum of the American Helicopter Society, New Orleans, LA, May 17-20, 1981, pp. 188-203.

5. Johnson, W., "Self-Tuning Regulators for Multicyclic Control of Helicopter Vibration," NASA TP 1996, March 1982.

6. Davis, M. W., "Refinement and Evaluation of Helicopter Real-Time Self-Adaptive Active Vibration Controller Algorithms," NASA CR 3821, August 1984.

7. Hall, S. R., and Wereley, N. M., "Linear Control Issues in the Higher Harmonic Control of Helicopter Vibrations," Proceedings of the 45th Annual Forum of the American Helicopter Society, Boston, MA, May 22-24, 1989, pp. 955-971.

8. Nixon, M.W.; Kvaternik, R.G.; and Settle, T.B., "Tiltrotor Vibration Reduction Through Higher Harmonic Control," 53rd Annual Forum of the American Helicopter Society, Virginia Beach, VA, May 1997.

9. Settle, T. B.; and Kidd, D. L., "Evolution and Test History of the V-22 0.2-Scale Aeroelastic Model," Journal of the American Helicopter Society, Vol. 37, No. 1, January 1992, pp. 31-45.

10. Corso, L.M.; Popelka, D.A.; and Nixon, M.W., "Design, Analysis, and Test of a Composite Tailored Tiltrotor Wing," 53rd Annual Forum of the American Helicopter Society, Virginia Beach, VA, May 1997.

11. Shaw, J., Albion, N., Hanker, E. J., Jr., and Teal, R. S., "Higher Harmonic Control: Wind Tunnel Demonstration of Fully Effective Vibratory Hub Force Suppression," Journal of the American Helicopter Society, Vol. 34, No. 1, January 1989, pp. 14-25.

12. Settle, T.B.; and Nixon, M.W., "MAVSS Control of an Active Flaperon for Tiltrotor Vibration Reduction," 53rd Annual Forum of the American Helicopter Society, Virginia Beach, VA, May 1997.